

Integrals of Products of Bessel Functions: An Insight from the Physics of Bloch Electrons

J. Covey¹ and D. L. Maslov¹

Department of Physics, University of Florida, Gainesville, FL 32611-8440, USA

(*Electronic mail: jcovey@ufl.edu)

(Dated: August 16, 2024)

Integrals of products of Bessel functions exhibit an intriguing feature: under certain conditions on the parameters specifying the integrand, they vanish identically. We provide a physical interpretation of this feature in the context of both single-particle and many-body properties of electrons on a lattice ("Bloch electrons"), namely, in terms of their density of states and umklapp scattering rate. (In an umklapp event, the change in the momentum of two colliding electrons is equal to a reciprocal lattice vector, which gives rise to a finite resistivity due to electron-electron interaction.) In this context, the vanishing of an integral follows simply from the condition that either the density of states vanishes due to the electron energy lying outside the band in which free propagation of electron waves is allowed, or that an umklapp process is kinematically forbidden due to the Fermi surface being smaller than a critical value.

I. INTRODUCTION

Bessel functions appear time and again in mathematics, physics, and engineering. The subject of this paper is a particular property of integrals of products of Bessel functions to vanish for a whole range of parameters. Various integrals of this kind were investigated via ingenious use of contour integral techniques by 19th century mathematicians, such as Hankel, Sonine, Weber, and Gegenbauer, to name a few, and later presented in Watson's seminal text on Bessel functions¹. More examples, involving both cylindrical and spherical Bessel functions, were studied in more recent works²⁻⁶.

The most general form of such integrals for cylindrical Bessel functions of the first kind may be written as

$$f(\{c_n\}) = \int_0^\infty d\rho \rho^{\alpha-1} \prod_{n=1}^{M>1} J_{\nu_n}(c_n \rho), \quad (1)$$

where the coefficients c_n are real and positive, and ordered such that $c_1 \leq c_2 \leq \dots \leq c_{M-1} < c_M$, while the "dimensionality" α and indices ν_n may take arbitrary, including complex, values. (If α is real, it can indeed be viewed as the dimensionality of some abstract geometrical space, but we will be using the same term even for an arbitrary α .) The integral (1) is convergent if $-\sum_{n=1}^M \text{Re } \nu_n < \text{Re } \alpha < M/2 + 1$. The result for the integral depends crucially on two relations between the input parameters. The first one, which we will be referring to as the "polygonal constraint", reads

$$c_M < \sum_{n=1}^{M-1} c_n, \quad (2)$$

in which case the coefficients c_n can be viewed as the sides of a planar polygon, see Fig. 1. The second one, which we will be referring to as the "charge neutrality condition", is given by

$$\nu_M = \sum_{n=1}^{M-1} \nu_n + \alpha - 2m; \quad m = 1, 2, 3, \dots \quad (3)$$

If we assign a fictitious "charge" ν_n to the n^{th} side of the polygon, the condition (3) says that the charge on the M^{th} side must be equal to the sum of the charges on other sides, modulo the integration dimensionality and a negative, even integer.

A closed-form solution of Eq. (1) for the case when the polygonal constraint (2) is *not* satisfied can be found in the monumental tables by Prudnikov, Brychkov, and Marichev⁷:

$$f(\{c_n\}) = \begin{cases} 2^{\alpha-1} c_M^{\nu_M-\mu} \frac{\Gamma(\mu/2)}{\Gamma(\nu_M-\mu/2+1)} \prod_{n=1}^{M-1} \frac{c_n^{\nu_n}}{\Gamma(\nu_n+1)} \\ \quad \times F_C^{(M-1)}\left(\frac{\mu}{2}, \frac{\mu}{2} - \nu_M; \nu_1 + 1, \dots, \nu_{M-1} + 1; \frac{c_1^2}{c_M^2}, \dots, \frac{c_{M-1}^2}{c_M^2}\right), & \text{if (3) is false;} \\ 0, & \text{if (3) is true,} \end{cases} \quad (4)$$

where $\mu = \alpha + \sum_{n=1}^M \nu_n$ and $F_C^{(N)}(a, b; x_1, \dots, x_N; y_1, \dots, y_N)$ is the "type C" Lauricella hypergeometric function. The null result in the second line of Eq. (4) follows from the first line, for when Eq. (3) is satisfied the gamma function $\Gamma(\nu_M - \mu/2 + 1) = \Gamma(-m + 1)$

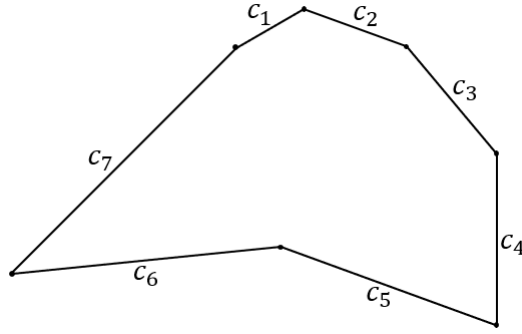


Figure 1: An illustration of the constraint (2) for a seven-sided polygon with sides satisfying $c_1 < c_2 \dots c_6 < c_7$.

has a pole. If the polygonal constraint is satisfied, there is no general closed-form of the integral (1), except for $M = 2, 3, 4$ and then for some special choices of ν_n and α , considered by Sonine⁸, Nicholson⁹, and Watson¹.

The peculiar, yet sublime, emergence of the geometric constraint (2) in tandem with the charge-neutrality condition (3) appears in a variety of seemingly different physical problems for the particular case of integrals over products of integer- or half-integer-order Bessel functions. It is in these cases that the integrand can be expressed in terms of δ -functions, a tool 19th century mathematicians did not have at their disposal. Integrals of the same form as (1) with $\nu_n \in \mathbb{Z}$ and $\nu_n + 1/2 \in \mathbb{Z}$ arise in a variety of settings. In particular, they have been analyzed by Jackson and Maximon² with the help of δ -functions for the special case of $M = 3$ and either $\nu_n \in \mathbb{Z}$ in two dimensions or $\nu_n + 1/2 \in \mathbb{Z}$ in three dimensions. Mehrem³⁻⁵ considered analytical solutions to integrals of products of up to four spherical Bessel functions, arising in the context of nuclear scattering. Integrals of the same form as (1) may also be found in other unsuspected places, such as in the random-walk problem⁶.

A similar class of integrals involves a product of trigonometric and Bessel functions, e.g.,

$$g(\{c_n\}) = \int_0^\infty d\rho \rho^{\alpha-1} [A \cos(c_M \rho) + B \sin(c_M \rho)] \prod_{n=1}^{M-1} J_{\nu_n}^{M-1}(c_n \rho). \quad (5)$$

Integrals of this type were studied in the random-walk problem⁶. To the best of our knowledge, explicit results are known only for $M = 2, 3$ ⁷. In particular, for $B = 0$, $M = 3$, $\alpha = 1$ and $\nu_1 = \nu_2$, the integral is non-zero only if the polygonal constraint (2) is satisfied, i.e., $c_3 < c_1 + c_2$, in which case the result is expressed via the complete elliptic integrals.

The vanishing of the integrals (1) and (5) for a whole range of parameters is an interesting phenomenon, particularly because it does not follow from any orthogonality condition. The goal of this paper is to give a physical interpretation of this phenomenon in the context of properties of electrons on a lattice ("Bloch electrons").

In the absence of interaction, the electron wavefunction satisfies the Bloch theorem¹⁰

$$\psi_{n\mathbf{k}}(\mathbf{r} + \mathbf{R}) = e^{i\mathbf{k} \cdot \mathbf{R}} \psi_{n\mathbf{k}}(\mathbf{r}), \quad (6)$$

where \mathbf{R} is any lattice vector and the quasimomentum \mathbf{k} is defined up to an arbitrary reciprocal lattice vector \mathbf{G} , the latter satisfying the condition $e^{i\mathbf{G} \cdot \mathbf{R}} = 1$. The unit cells of the reciprocal lattice are known as Brillouin zones and, conventionally, one considers physically nonequivalent quasimomenta within the first Brillouin zone. An electron can propagate through the lattice only if its energy lies within one of the bands, which are separated by forbidden energy gaps. An all important property of the electron spectrum is the density of states

$$\nu(E) = \int \frac{d^D k}{(2\pi)^D} \delta(E - \varepsilon_{\mathbf{k}}), \quad (7)$$

where $\varepsilon_{\mathbf{k}}$ is the electron dispersion within a given band. Naturally, $\nu(E)$ is non-zero only if E is within the band, and zero otherwise. Already this simple property allows one to see a physical example of the polygonal constraint for integrals of the type (5).

We illustrate our approach for the simplest lattice model—the tight-binding model—in which electron hopping is allowed only between a limited number of nearest neighbors. For example, the energy spectrum of electrons for a square lattice with nearest-neighbor hopping is given by¹¹

$$\varepsilon_{\mathbf{k}} = -t (\cos k_x + \cos k_y), \quad -\pi \leq k_x, k_y \leq \pi, \quad (8)$$

where we have set the lattice constant to unity, t is the "hopping amplitude", and the first Brillouin zone is a square of side π . The band spans the interval of energies from $-2t$ to $2t$, such that the density of states is non-zero only if $-2t < E < 2t$. To see

how it is relevant to the integral (5), we replace the δ -functions in Eq. (7) by its integral representation and swap the order of integration:

$$v(E) = \int_{-\infty}^{\infty} d\rho e^{iE\rho} \int \frac{dk_x}{2\pi} e^{i\rho t \cos k_x} \int \frac{dk_y}{2\pi} e^{i\rho t \cos k_y}. \quad (9)$$

Using the integral representation of a Bessel function of integer order

$$J_n(z) = \frac{1}{2\pi i^n} \int_0^{2\pi} d\phi e^{i(z \cos \phi \pm n\phi)}, \quad (10)$$

we obtain

$$v(E) = 2 \int_0^{\infty} d\rho \cos(E\rho) J_0^2(t\rho) = \frac{2}{\pi t} \Theta(2t - |E|) \mathbb{K} \left(\sqrt{1 - \left(\frac{E}{2t}\right)^2} \right), \quad (11)$$

which is the special case of Eq. (5) with $B = 0$, $\alpha = 1$, $M = 3$, $c_3 = E$, $v_1 = v_2 = 0$, and $c_1 = c_2 = t$. Here, $\mathbb{K}(x)$ is the complete elliptic integral of the first kind. Now we see that the polygonal constraint is nothing but the condition for the energy to lie within the band. (Although we chose all $c_n > 0$, the integral (11) is obviously an even function of E , such that the interval $-2t < E < 0$ does not require a special consideration.) In what follows, we show that the integral (5) vanishes for any M , $\alpha = 1$, and under certain conditions on v_n 's, by considering the density of states and conductivity of electrons on a hyperrectangular lattice in $D = M - 1$ dimensions.

The integral (1) occurs in a more complex physical context of mutual scattering of Bloch electrons. In contrast to the real momentum, which is conserved in electron-electron scattering in the absence of a lattice, the quasimomentum is conserved only up to an arbitrary reciprocal lattice vector. The relation between initial momenta $\mathbf{k}_1 \dots \mathbf{k}_N$ and final momenta $\mathbf{k}'_1 \dots \mathbf{k}'_N$ in an N -electron collision can be written as

$$\sum_{n=1}^N (\mathbf{k}'_n - \mathbf{k}_n) = \mathbf{G}. \quad (12)$$

If $\mathbf{G} = 0$, the scattering process is called "normal". If $\mathbf{G} \neq 0$, it is called "umklapp" (from German "umklappen", which means "fold down" in English). In the latter case, at least one of the final momenta lies outside of the first Brillouin zone, but it can be translated back ("folded fown") to this zone via a shift by \mathbf{G} . A very important distinction between normal and umklapp scattering processes is that only the latter can render the electrical resistivity of a metal finite, even in the absence of electron scattering by disorder and phonons¹². Due to the Pauli exclusion principle, scattering affects only electrons with energies in a narrow window near the Fermi energy (E_F), of width set by the thermal energy, T . (Hereinafter, we set $k_B = 1$.) For a two-electron collision, this implies that the scattering rate, and thus the resistivity, are proportional to T^2 .

Since the quasimomenta of electrons are confined to the Fermi surface, the condition (12) for an umklapp scattering process can be satisfied only if the Fermi surface is sufficiently large. Namely, the umklapp scattering rate is equal to zero if

$$\left| \sum_{n=1}^N (\mathbf{k}'_n - \mathbf{k}_n) \right|_{\mathbf{k}_1 \dots \mathbf{k}_N, \mathbf{k}'_1 \dots \mathbf{k}'_N \in \text{FS}} < G_0, \quad (13)$$

where G_0 is the magnitude of the shortest non-zero reciprocal lattice vector, which is on the order of the inverse interatomic distance. The condition (13) is reminiscent of the polygonal constraint (2), and the vanishing of the umklapp scattering rate is reminiscent of the analogous property of the integral (1). This is the basis of our physical interpretation.

The rest of the paper is organized as follows. In Sec. II, we consider the density of states and conductivity of electrons on a D -dimensional lattice, thereby proving the polygonal constraint for a certain class of the integrals of type (5). In Sec. III, we show that integrals of the form (1) do appear in the umklapp scattering rate with $M = 2N + 1$, integer or half-integer v_n , and $\alpha = 2$ or $\alpha = 3 - M/2$ for 2D and 3D lattices, respectively, if the actual Fermi surfaces are replaced by circles in 2D and spheres in 3D. In Secs. III A and III B, we consider a particular example of two-electron umklapp scattering on a 2D honeycomb lattice, encountered, e.g., in graphene¹³. N -electron scattering processes on 2D and 3D lattices are analyzed in Secs. III C and III E, respectively. The threshold behavior of the scattering rate just above the threshold for umklapp scattering is derived in Sec. III D. In Sec. IV, we consider more mathematical aspects of the charge-neutrality condition (3). A detailed derivation of the umklapp scattering rate and further mathematical details are delegated to the supplementary material.

II. SINGLE-PARTICLE PROPERTIES OF BLOCH ELECTRONS ON A D -DIMENSIONAL LATTICE

In this section we analyze Eq. (5), using some properties of Bloch electrons on a hyperrectangular lattice in $D = M - 1$ dimensions. Such a lattice is formed by D orthogonal vectors of length a_n , and we assume that electrons can hop only between nearest neighbors with amplitude t_n in the n^{th} direction. Analogous to the 2D case [cf. Eq. (8)], the electron energy spectrum is given by

$$\varepsilon_{\mathbf{k}} = - \sum_{n=1}^{M-1} t_n \cos(k_n a_n), \quad (14)$$

and the band spans an energy interval $(-\sum_{n=1}^{M-1} t_n, \sum_{n=1}^{M-1} t_n)$. The corresponding Brillouin zone is also a hyperrectangle with sides $2\pi/a_n$. Following the same steps that lead us to Eq. (11), we obtain for the density of states

$$\begin{aligned} \nu(E) &= \prod_{n=1}^{M-1} \int_{-\pi/a_n}^{\pi/a_n} \frac{dk_n}{2\pi} \delta\left(E - \sum_{n=1}^{M-1} t_n \cos(k_n a_n)\right) \\ &= 2 \prod_{n=1}^{M-1} a_n^{-1} \int_0^\infty d\rho \cos(E\rho) \prod_{n=1}^{M-1} J_0(t_n \rho), \end{aligned} \quad (15)$$

which is non-zero only if $|E| < \sum_{n=1}^{M-1} t_n$. Therefore, we have proven that the integral (5) is non-zero only if Eq. (2) is satisfied for arbitrary M , provided that $B = 0$ and $\nu_1 = \dots = \nu_{M-1} = 0$.

In the context of Bloch electrons, the Bessel functions of non-zero (but integer) order occur in calculating averages of the projections of momenta or velocities. For example, the conductivity in the presence of short-range disorder, characterized by the mean free time τ_d , is given by¹⁰

$$\sigma_{ij}(E_F) = 2e^2 \tau_d \prod_{n=1}^{M-1} \int_{-\pi/a_n}^{\pi/a_n} \frac{dk_n}{2\pi} \delta\left(E_F - \sum_{n=1}^{M-1} t_n \cos(k_n a_n)\right) v_i v_j, \quad (16)$$

where $v_n = \partial \varepsilon_{\mathbf{k}} / \partial k_n = t_n a_n \sin(k_n a_n)$ is the n^{th} Cartesian component of the group velocity. With the help of Eq. (10), we obtain for the diagonal component of the conductivity

$$\sigma_{jj}(E_F) = e^2 \tau_d (t_j a_j)^2 [\nu(E_F) + 2I(E_F)], \quad (17)$$

where $\nu(E_F)$ is the density of states in Eq. (15) evaluated at $E = E_F$, and

$$I(E_F) = \prod_{n=1}^{M-1} a_n^{-1} \int_0^\infty d\rho \cos(E_F \rho) J_2(t_j \rho) \prod_{n=1, n \neq j}^{M-1} J_0(t_n \rho). \quad (18)$$

From its definition in Eq. (16), we see that $\sigma_{jj}(E_F) \neq 0$ only if $|E_F| < \sum_{n=1}^{M-1} t_n$. The first term in Eq. (17) itself obeys this rule. Therefore, the integral (18) must also obey this rule.

In general, we consider the integral (5) with $\alpha = 1$, subject to additional constraints: namely, ν_n are integers, such that i) $\sum_{n=1}^{M-1} \nu_n = 2p$ and $B = 0$ or ii) $\sum_{n=1}^{M-1} \nu_n = 2p + 1$ and $A = 0$, with $p = 0, 1, 2, \dots$. In both cases, the product of the Bessel functions is an even function of ρ , and the integral over ρ can be extended over the entire real axis. By working backwards through steps in the previous examples, we obtain for case i),

$$\begin{aligned} g(\{c_n\}) &= \frac{1}{2} \text{Re} \int_{-\infty}^\infty d\rho e^{-ic_M \rho} \prod_{n=1}^{M-1} \int \frac{dk_n}{2\pi i^{\nu_n}} e^{i(\rho c_n \cos k_n + \nu_n k_n)} \\ &= \frac{(-1)^p}{2} \prod_{n=1}^{M-1} \int \frac{dk_n}{2\pi} \delta\left(c_M - \sum_{n=1}^{M-1} c_n \cos k_n\right) \cos\left(\sum_{n=1}^{M-1} \nu_n k_n\right). \end{aligned} \quad (19)$$

The polygonal constraint now follows simply from $c_M = \sum_{n=1}^{M-1} c_n \cos k_n \leq \sum_{n=1}^{M-1} c_n$. Case ii) is analyzed in the same way, with Re in Eq. (19) replaced by Im.

III. UMKLAPP SCATTERING OF BLOCH ELECTRONS

A. Example: Two-particle umklapp scattering on a honeycomb lattice

To provide the physical context for the integral (1), we start with a simple example of two-electron scattering on a 2D honeycomb lattice, encountered, e.g., in graphene. As depicted in Fig. 2a, the reciprocal lattice is also a honeycomb. The first Brillouin zone

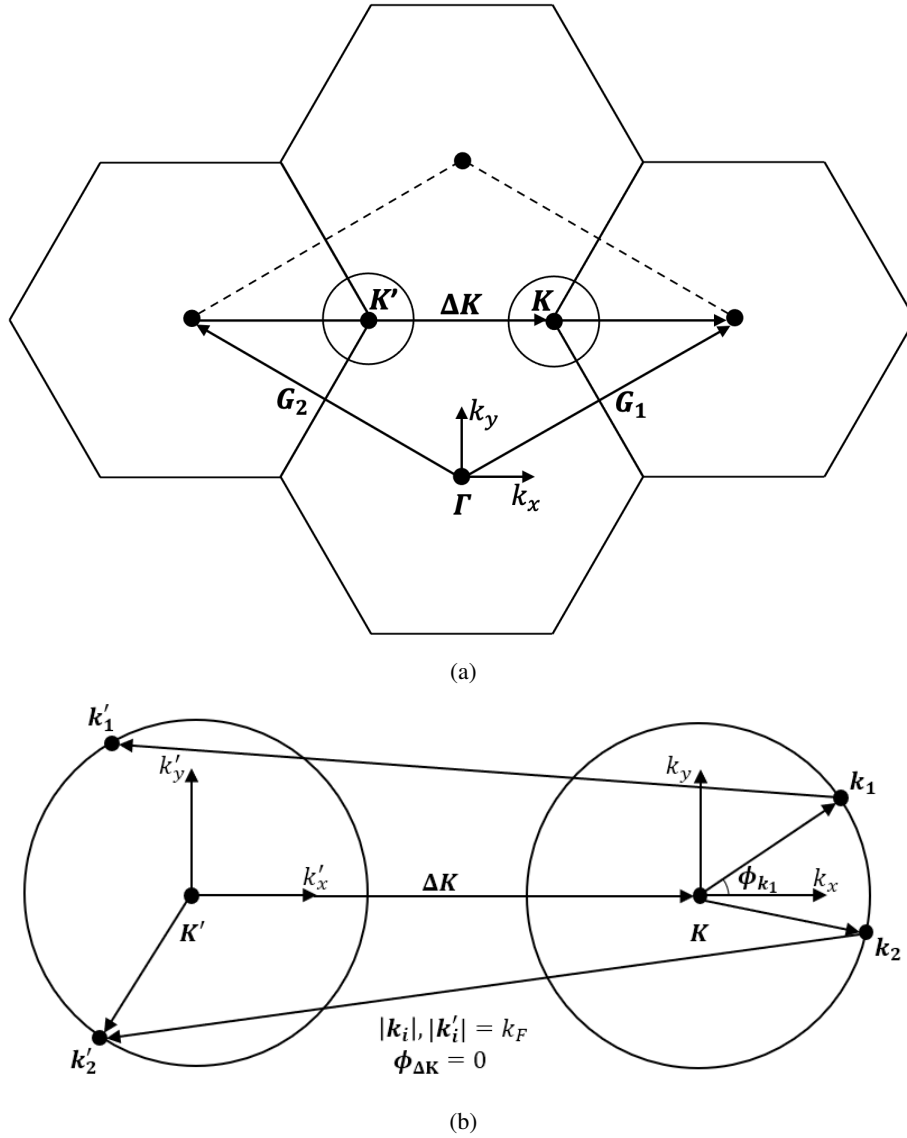


Figure 2: (a) The reciprocal lattice of a real-space honeycomb lattice in real space is also a honeycomb lattice. \mathbf{K} and \mathbf{K}' points are the degeneracy points of the electron spectrum. The Brillouin zone is defined by the region enclosed by \mathbf{G}_1 and \mathbf{G}_2 and the two dashed lines. (b) An example of a two-particle intervalley scattering process: electrons with initial momenta \mathbf{k}_1 and \mathbf{k}_2 (measured relative to the \mathbf{K} point) scatter into the states with momenta \mathbf{k}'_1 and \mathbf{k}'_2 (measured relative to the \mathbf{K}' point) on the Fermi surface around the \mathbf{K}' point. A scattering process can lead to an umklapp only if $4k_F \geq |\Delta\mathbf{K}|$. The model is applicable as long as the Fermi surfaces do not overlap, i.e., for $2k_F < |\Delta\mathbf{K}|$.

may be defined by the reciprocal lattice vectors \mathbf{G}_1 and \mathbf{G}_2 and contains two nonequivalent corner points, \mathbf{K} and \mathbf{K}' . A special feature of the honeycomb lattice is that the electron energy spectrum is doubly degenerate (in addition to spin degeneracy) at the corner points. Near these points, the spectrum is that of massless Dirac fermions: $\varepsilon_{\mathbf{k}} = \pm v_F k$, where v_F is the (k -independent) Fermi velocity and \pm corresponds to the conduction/valence bands¹³. The full dispersion of electrons in graphene and a zoomed view of the Dirac cones are depicted in Fig. 3a. (The lattice constant and hopping parameter were set to unity). In Fig. 3b, the isoenergetic contours are plotted at two different energies. At lower energies, the Fermi surfaces are nearly isotropic, while at higher energies the contours display more noticeable trigonal warping.

If the Fermi energy is either above or below the touching points of two Dirac cones, the system is a metal with a Fermi surface that consists of two contours ("valleys") centered at the \mathbf{K} and \mathbf{K}' points. (Without loss of generality, we will assume that the Fermi level is at energy E_F above the touching point.) At lower fillings, when the size of the valleys is much smaller than the reciprocal lattice vector, the valleys are almost circular, as depicted in Fig. 2a. At higher fillings, the valleys get (trigonally)

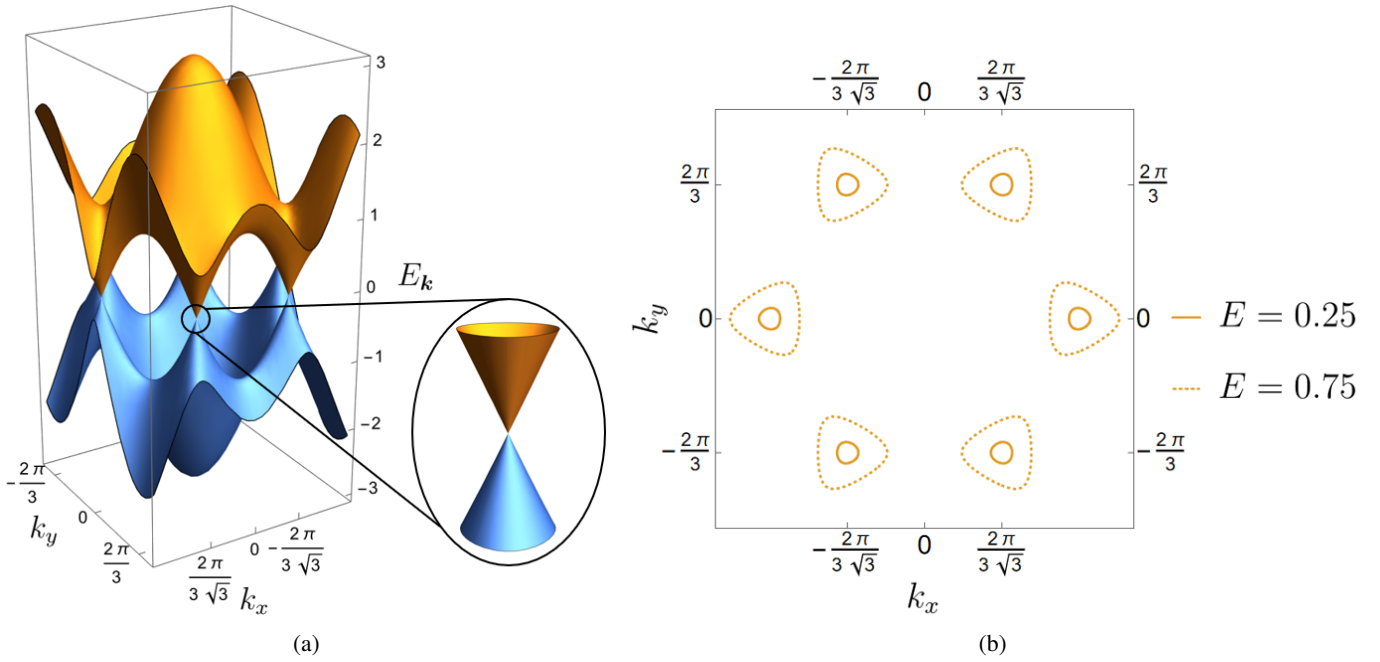


Figure 3: (a) The full dispersion of electrons in graphene obtained from the nearest-neighbor tight-binding model¹³. Encircled is a zoomed in view of the Dirac cones (with finite trigonal warping) centered about a \mathbf{K} point. (b) Fermi surface contours for two different energies (in units of the hopping parameter).

distorted; however, we are going to ignore this in our simple model. As we said in Sec. I, umklapp events require large changes in the total quasimomentum of the colliding electrons. For a two-valley system, the largest change in the momentum is achieved when two electrons are transferred simultaneously from one valley to another. Simple geometry shows that the vector $\Delta\mathbf{K}$ connecting the \mathbf{K} and \mathbf{K}' points is given by $\Delta\mathbf{K} = \mathbf{K} - \mathbf{K}' = (\mathbf{G}_1 - \mathbf{G}_2)/3$. On the other hand, any superposition of the lattice vectors is also a lattice vector, and thus $\mathbf{G} = \mathbf{G}_1 - \mathbf{G}_2 = 3\Delta\mathbf{K}$ is a lattice vector as well. If the electron momenta in each valley are measured from the valley centers, a two-electron intervalley transfer becomes an umklapp event if

$$\mathbf{k}_1 + \mathbf{k}_2 - \mathbf{k}'_1 - \mathbf{k}'_2 + 2(\mathbf{K} - \mathbf{K}') > \mathbf{G}_1 - \mathbf{G}_2 \quad (20)$$

or

$$\mathbf{k}_1 + \mathbf{k}_2 - \mathbf{k}'_1 - \mathbf{k}'_2 > \Delta\mathbf{K}. \quad (21)$$

As shown in Fig. 2b, we consider two electrons initially in the \mathbf{K} valley that scatter to the \mathbf{K}' valley. For circular valleys of radii k_F , the magnitude of the left-hand side of Eq. (21) is maximized when two electrons are transferred from, say, the rightmost edge of valley \mathbf{K} to the leftmost edge of valley \mathbf{K}' , such that $|\mathbf{k}_1 + \mathbf{k}_2 - \mathbf{k}'_1 - \mathbf{k}'_2| = 4k_F$. Therefore, umklapps are possible for $k_F > \Delta K/4 = G/12$, i.e., when k_F is still sufficiently small compared to G . *A posteriori*, this serves as a justification (albeit only a numerical one) for neglecting the trigonal distortion of the Fermi surface. On the other hand, the valleys touch each other at $k_F = \Delta K/2$, after which the model becomes meaningless. (For a real honeycomb lattice, the Fermi surface undergoes a reconstruction at some critical filling, when a new pocket is opened at the center of the Brillouin zone). Thus, the relevant range for umklapp scattering is $\Delta K/4 \leq k_F < \Delta K/2$.

The scattering rate of an electron with momentum \mathbf{k}_1 due to an umklapp process is given by the Fermi Golden Rule

$$\frac{1}{\tau_{\mathbf{k}_1}} = \int \frac{d^2 k_2}{(2\pi)^2} \int \frac{d^2 k'_1}{(2\pi)^2} \int \frac{d^2 k'_2}{(2\pi)^2} W_{\mathbf{k}_1, \mathbf{k}_2; \mathbf{k}'_1, \mathbf{k}'_2} \left[n_{\mathbf{k}_2} (1 - n_{\mathbf{k}'_1}) (1 - n_{\mathbf{k}'_2}) + n_{\mathbf{k}'_1} n_{\mathbf{k}'_2} (1 - n_{\mathbf{k}_2}) \right] \times \delta(\mathbf{k}_1 + \mathbf{k}_2 - \mathbf{k}'_1 - \mathbf{k}'_2 - \Delta\mathbf{K}) \delta(\varepsilon_{\mathbf{k}_1} + \varepsilon_{\mathbf{k}_2} - \varepsilon_{\mathbf{k}'_1} - \varepsilon_{\mathbf{k}'_2}), \quad (22)$$

where $W_{\mathbf{k}_1, \mathbf{k}_2; \mathbf{k}'_1, \mathbf{k}'_2}$ is the scattering probability density, $n_{\mathbf{k}}$ is the Fermi function, and $\varepsilon_{\mathbf{k}}$ is the electron energy. For our purposes, the screened Coulomb interaction between electrons can be replaced by a δ -function potential with amplitude u . In this case, we have (see Secs. I-II of the supplementary material for details)

$$W_{\mathbf{k}_1, \mathbf{k}_2; \mathbf{k}'_1, \mathbf{k}'_2} = 16\pi u^2 \sin^2\left(\frac{\phi_1 + \phi'_1}{2}\right) \sin^2\left(\frac{\phi_2 + \phi'_2}{2}\right), \quad (23)$$

where ϕ_1 is the azimuthal angle of \mathbf{k}_1 , etc. The angular dependence of $W_{\mathbf{k}_1, \mathbf{k}_2; \mathbf{k}'_1, \mathbf{k}'_2}$ comes from the spinor structure of the wavefunctions of the Dirac Hamiltonian. It is convenient to choose $|\mathbf{k}_1| = k_F$ and average $1/\tau$ over the directions of \mathbf{k}_1 . In doing so, we obtain for the averaged scattering rate at $T \ll E_F$,

$$\left\langle \frac{1}{\tau} \right\rangle = \frac{\pi}{2} \lambda^2 \frac{T^2}{E_F} f(c), \quad (24)$$

where $\lambda = k_F u / v_F$ is a dimensionless coupling constant, $c = \Delta K / k_F$, $f(c) = S_1(c) - 2S_2(c) + S_3(c)$, and

$$S_j(c) = \frac{1}{(2\pi)^5} \int_0^{2\pi} d\phi'_1 \int_0^{2\pi} d\phi'_2 \int_0^{2\pi} d\phi_1 \int_0^{2\pi} d\phi_2 \delta(\cos \phi'_1 + \cos \phi'_2 - \cos \phi_1 - \cos \phi_2 - c \cos \phi_{\Delta\mathbf{K}}) \\ \times \delta(\sin \phi'_1 + \sin \phi'_2 - \sin \phi_1 - \sin \phi_2 - c \sin \phi_{\Delta\mathbf{K}}) R_j, \quad j = 1, 2, 3 \quad (25)$$

with $R_1 = 1$, $R_2 = \cos(\phi_1 + \phi'_1)$, and $R_3 = \cos(\phi_1 + \phi'_1) \cos(\phi_2 + \phi'_2)$. In the last equation, the δ -functions of momentum conservation were re-written in terms of the Cartesian components of the total quasimomentum. Although in our geometry vector $\Delta\mathbf{K}$ has only an x -component, we allowed also for possible y -components for the sake of generality. This completes the prelude from condensed matter physics.

B. Integrals of products of Bessel functions for two-particle umklapp scattering

Now we will show that the integral in Eq. (25) is, indeed, a special case of Eq. (1). First, we re-write the δ -functions in Eq. (25) as

$$\delta(r) = \int_{-\infty}^{\infty} dx e^{ixr}, \quad (26)$$

such that

$$S_j(c) = \frac{1}{(2\pi)^5} \int_{-\infty}^{\infty} dx \int_{-\infty}^{\infty} dy \int_0^{2\pi} d\phi'_1 \int_0^{2\pi} d\phi'_2 \int_0^{2\pi} d\phi_1 \int_0^{2\pi} d\phi_2 \\ \times e^{ix(\cos \phi'_1 + \cos \phi'_2 - \cos \phi_1 - \cos \phi_2 - c \cos \phi_{\Delta\mathbf{K}})} e^{iy(\sin \phi'_1 + \sin \phi'_2 - \sin \phi_1 - \sin \phi_2 - c \sin \phi_{\Delta\mathbf{K}})} R_j. \quad (27)$$

The Cartesian coordinates may be transformed to polar ones such that $x = \rho \cos \varphi$ and $y = \rho \sin \varphi$, giving

$$x \cos \phi + y \sin \phi = \rho(\cos \varphi \cos \phi + \sin \varphi \sin \phi) = \rho \cos(\phi - \varphi) \quad (28)$$

for all $\phi = \phi_1, \dots, \phi'_2, \phi_{\Delta\mathbf{K}}$. For S_1 with $R_1 = 1$, we then obtain

$$S_1(c) = \frac{1}{(2\pi)^5} \int_0^{\infty} d\rho \rho \int_0^{2\pi} d\varphi \int_0^{2\pi} d\phi'_1 \int_0^{2\pi} d\phi'_2 \int_0^{2\pi} d\phi_1 \int_0^{2\pi} d\phi_2 \\ \times e^{i\rho(\cos(\phi'_1 - \varphi) + \cos(\phi'_2 - \varphi) - \cos(\phi_1 - \varphi) - \cos(\phi_2 - \varphi) - c \cos(\phi_{\Delta\mathbf{K}} - \varphi))}. \quad (29)$$

The integrations over $\phi_1 \dots \phi'_2$ are carried out independently from each other as each such integration goes over the full period of the integrand and therefore does not depend on φ . Using the integral representation of a Bessel function of integer order, Eq. (10), we have

$$S_1(c) = \frac{1}{2\pi} \int_0^{\infty} d\rho \rho J_0^4(\rho) \int_0^{2\pi} d\varphi e^{-ic\rho \cos(\phi_{\Delta\mathbf{K}} - \varphi)}. \quad (30)$$

Applying Eq. (10) again, we obtain

$$S_1(c) = \int_0^{\infty} d\rho \rho J_0^4(\rho) J_0(c\rho). \quad (31)$$

The remaining two integrals in Eq. (25), S_2 and S_3 , differ from S_1 only in the additional angular dependence of factors R_2 and R_3 . Following the same steps as before, we obtain

$$S_2(c) = -\cos(2\phi_{\Delta\mathbf{K}}) \int_0^{\infty} d\rho \rho J_0^2(\rho) J_1^2(\rho) J_2(c\rho) \quad (32)$$

and

$$S_3(c) = \frac{\cos(4\phi_{\Delta\mathbf{K}})}{2} \int_0^\infty d\rho \rho J_1^4(\rho) J_4(c\rho) + \frac{1}{2} \int_0^\infty d\rho \rho J_1^4(\rho) J_0(c\rho). \quad (33)$$

We see that Eqs. (31)-(33) are indeed special cases of Eq. (1) with $M = 5$, $\alpha = 2$, $c_1 = \dots = c_4 = 1$, and $c_5 = c$, such that the corresponding polygon, defined by Eq. (2), is a pentagon with the four shorter sides being of the same length. The indices of the Bessel functions in all three equations are such that the charge-neutrality condition (3) is satisfied. For S_1 , $\nu_1 = \dots = \nu_5 = 0$ such that Eq. (3) is satisfied with $m = 1$:

$$\nu_5 = 0 = 4 \times 0 + 2 - 2 \times 1. \quad (34)$$

For S_2 , $\nu_1 = \nu_2 = 0$, $\nu_3 = \nu_4 = 1$, and $\nu_5 = 2$, such that Eq. (3) is also satisfied with $m = 1$

$$\nu_5 = 2 = 2 \times (0 + 1) + 2 - 2 \times 1. \quad (35)$$

Likewise, it is easy to check that for the first and second terms of S_3 , Eq. (3) is satisfied with $m = 1$ and $m = 3$, respectively.

Since Eq. (3) is satisfied, then, according to Eq. (4), all the integrals in Eq. (31)-(33) must vanish if Eq. (2) is *not* satisfied, i.e., if $c > 4$. Now we see why this is the case. Indeed, in our physical model $c = \Delta K/k_F$, hence $c > 4$ coincides with the condition $k_F < \Delta K/4$, when umklapp scattering is *forbidden*, and thus $f(c)$ in Eq. (24) must be equal to zero. This physical condition is enforced by the first δ -function in Eq. (22), and thus the somewhat mysterious mathematical property encoded by Eq. (4) allows for a simple interpretation in terms of momentum conservation.

The function $f(c)$ is plotted in Fig. 4 for $\phi_{\Delta\mathbf{K}} = 0$. (Although our physical model makes sense only for $c > 2$, when the valleys are separate, there are no mathematical constraints on the value of c .) In addition to the expected discontinuity of df/dc at $c = 4$, there are two other discontinuities at $c = 0$ and 2, the latter of which corresponds to the Fermi surfaces first touching. The discontinuities in the derivative are analyzed in Sec. III of the supplementary material. We will discuss the threshold behavior of $f(c)$ in Sec. III D, after generalizing our results for the case of N -particle scattering in the next section.

C. N -particle scattering on an abstract 2D lattice

In the previous section, we considered a particular model of Dirac fermions with two nonequivalent degeneracy points, which is the low-energy model of graphene. Some features of this model, such as the additional angular dependence of the scattering probability in Eq. (23), are specific for a given Hamiltonian. In this section, we take a more abstract approach and focus only on the constraints imposed by momentum conservation for an N -particle umklapp scattering process, without specifying a particular lattice model. We consider a hypothetical 2D Fermi surface consisting of N_{FS} concentric circles with radii $k_{F,1} \dots k_{F,N_{\text{FS}}}$, as shown in Fig. (5), and examine the case when N electrons, with initial momenta on any of the circles, scatter into their final states, also with momenta on any of the circles, such that the change in momentum matches the shortest reciprocal lattice vector \mathbf{G} . The initial and final states may be on the same or different circles. Momentum conservation is enforced via a δ -function

$$\delta\left(\sum_{n=1}^N (\mathbf{k}'_n - \mathbf{k}_n) - \mathbf{G}\right), \quad (36)$$

where the magnitude of each momentum is equal to the radius of one of the circles. The momenta may be rescaled to dimensionless ones such that $c_n = k'_n/k_{F,1}$ for odd n , $c_n = k_n/k_{F,1}$ for even n , and $c_{2N+1} = G/k_{F,1}$. Since the magnitude of each final and initial momentum is equal to one of the Fermi surface radii, $c_n = k_{F,n}/k_{F,1}$ both for even and odd n . If the scattering probability $W_{\mathbf{k}_1, \dots, \mathbf{k}_N; \mathbf{k}'_1, \dots, \mathbf{k}'_N}$ is replaced by a constant, the average scattering rate is proportional to the function

$$f(\{c_n\}) = \frac{1}{(2\pi)^{2N+1}} \prod_{n=1}^{2N} \int_0^{2\pi} d\phi_n \delta\left(\sum_{n=1}^{2N} (-1)^{n-1} c_n \cos \phi_n - c_{2N+1} \cos \phi_{2N+1}\right) \times \delta\left(\sum_{n=1}^{2N} (-1)^{n-1} c_n \sin \phi_n - c_{2N+1} \sin \phi_{2N+1}\right) \quad (37)$$

with $\{c_n\} = c_1, \dots, c_{2N+1}$. We can then follow the same procedure as for the two-particle case, i.e., replace the δ -functions by their integral forms and interchange the order of integration

$$f(\{c_n\}) = \frac{1}{(2\pi)^{2N+1}} \int_{-\infty}^{\infty} dx \int_{-\infty}^{\infty} dy \prod_{n=1}^{2N} \int_0^{2\pi} d\phi_n e^{ix(\sum_{n=1}^{2N} (-1)^{n-1} c_n \cos \phi_n - c_{2N+1} \cos \phi_{2N+1})} \times e^{iy(\sum_{n=1}^{2N} (-1)^{n-1} c_n \sin \phi_n - c_{2N+1} \sin \phi_{2N+1})}. \quad (38)$$

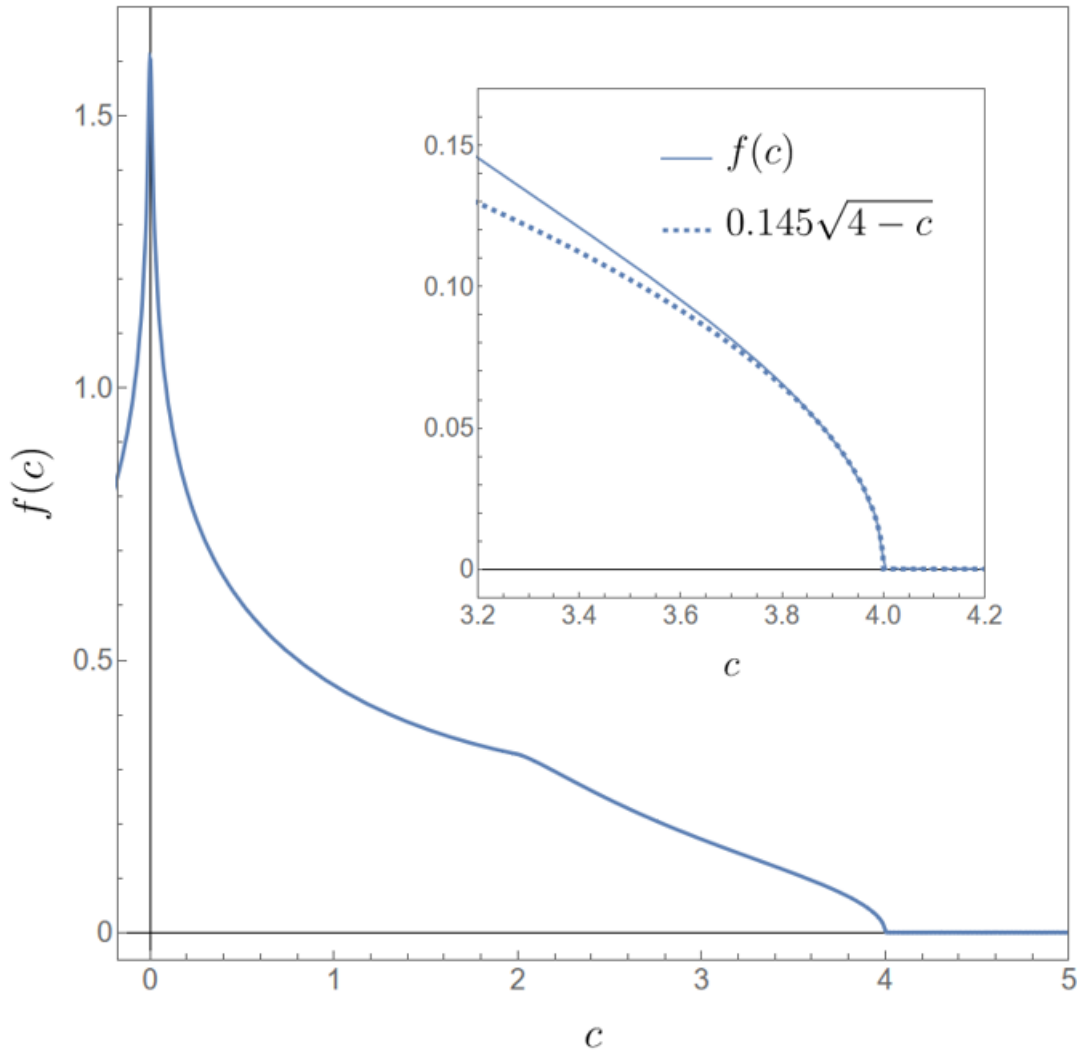


Figure 4: Main panel: Function $f(c)$ entering the average scattering rate due to two-particle umklapp scattering on a honeycomb lattice, Eq. (24). In this example, the polygonal constraint is satisfied if $c < 4$. Additional discontinuities in the derivative of $f(c)$ at $c = 0$ and $c = 2$ are discussed in Sec. II of the supplementary material. (Although the physical values of c are positive, we also showed a small region of negative c in order to emphasize the discontinuity of the derivative at $c = 0$.) Inset: closer view of $f(c)$ near the threshold at $c = 4$. As discussed in Sec. III D, $f(c)$ scales as $\sqrt{4-c}$ in the limit $c \rightarrow 4$ from below. The dashed line is a fit by the expression displayed in the legend.

Like arguments in the exponential terms may once again be combined and independently integrated as

$$\frac{1}{2\pi} \int_0^{2\pi} d\phi_n e^{\pm i c_n (x \cos \phi_n + y \sin \phi_n)} = J_0(c_n \rho), \quad (39)$$

leading to a product of Bessel functions, so that Eq. (38) is simplified to

$$f(\{c_n\}) = \frac{1}{2\pi} \int_0^\infty d\rho \rho \prod_{n=1}^{2N} J_0(c_n \rho) \int_0^{2\pi} d\varphi e^{-i c_{2N+1} (x \cos \phi_{2N+1} + y \sin \phi_{2N+1})} \quad (40)$$

The integration over φ reduces the last expression to the final form

$$f(\{c_n\}) = \int_0^\infty d\rho \rho \prod_{n=1}^{2N+1} J_0(c_n \rho), \quad (41)$$

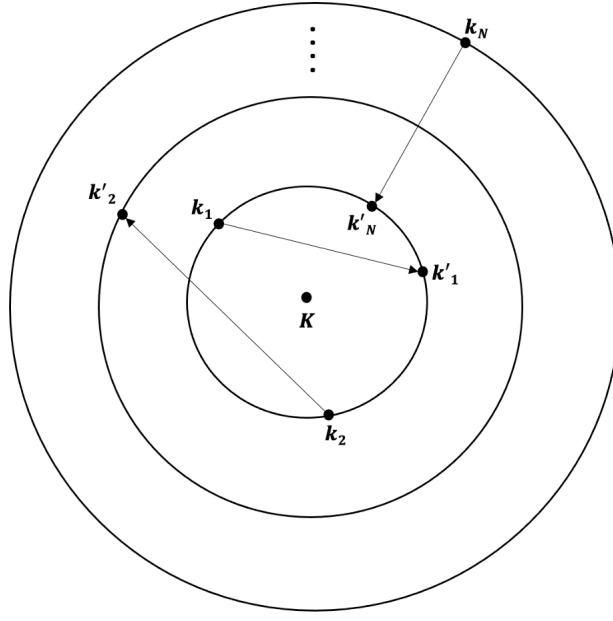


Figure 5: An example of an N -particle scattering event on a 2D Fermi surface, consisting of concentric circles. The N initial momenta $\mathbf{k}_{1\dots N}$ and N final momenta $\mathbf{k}'_{1\dots N}$ reside on concentric Fermi surfaces, with some possibly sharing the same Fermi surface.

which is again a special case of Eq. (1) with $M = 2N + 1$, $\alpha = 2$, and $\nu_1 = \dots = \nu_{2N+1} = 0$. The charge neutrality condition is clearly satisfied with $m = 1$, so that when the polygonal constraint is broken, namely $c_{2N+1} > \sum_{n=1}^{2N} c_n$, the integral vanishes. In terms of physical variables, the latter condition reads $\sum_{n=1}^{2N} k_{F,n} < G$, which means that the Fermi surfaces are too small to support an umklapp process. Again, the polygonal constraint is ensured by the structure of the δ -functions in Eqs. (36) and (37).

Bessel functions of non-zero orders arise due to the additional angular dependence of the scattering probability, $W_{\mathbf{k}_1, \dots, \mathbf{k}_N; \mathbf{k}'_1, \dots, \mathbf{k}'_N}$. In the realm of physical reality, such a dependence comes in the form of integer powers of trigonometric functions, $\cos \phi_n$ and $\sin \phi_n$, or, more generally, can be represented by infinite series of such functions. As in the two-particle case, additional factors of $\cos \phi_n$ and $\sin \phi_n$ will promote at least some of the indices of the Bessel functions to non-zero values. However, the indices will remain integer (or half-integer in 3D, cf. Sec. III E).

D. Threshold Behavior

If the polygonal constraint is satisfied, a closed-form result for the integral (1) is not known, except for some special cases. However, a representation of this integral in terms of δ -functions allows one to find the asymptotic behavior of the function $f(\{c_n\})$ just below the threshold for which the polygonal constraint (2) is no longer satisfied, i.e., for $c_{2N+1} = \sum_{n=1}^{2N} c_n - \epsilon$ with $0 < \epsilon \ll 1$. Setting $\phi_{2N+1} = 0$ for simplicity, we obtain instead of Eq. (37)

$$f(\{c_n\}) = \frac{1}{(2\pi)^{2N+1}} \prod_{n=1}^{2N} \int_0^{2\pi} d\phi_n \delta\left(\epsilon - \sum_{n=1}^{2N} c_n [1 - (-)^{n-1} \cos \phi_n]\right) \delta\left(\sum_{n=1}^{2N} c_n (-)^{n-1} \sin \phi_n\right). \quad (42)$$

For $\epsilon \ll 1$, the support of the integrals over ϕ_n comes from narrow regions near 0 (for odd n) and near π (for even n). Expanding $\cos \phi_{2p+1} = 1 - \phi_{2p+1}^2/2$, $\cos \phi_{2p} = \cos(\pi - \bar{\phi}_{2p}) = -1 + \bar{\phi}_{2p}^2/2$, $\sin \phi_{2p+1} = \phi_{2p+1}$, $\sin \phi_{2p} = \bar{\phi}_{2p}$, and extending the limits of integration to $\phi_{2p+1} \in (0, \infty)$ and $\phi_{2p} \in (-\infty, \infty)$, we have

$$f(\{c_n\}) \approx \frac{1}{(2\pi)^{2N+1}} \prod_{p=0}^{N-1} \int_0^\infty d\phi_{2p+1} \prod_{p=1}^N \int_{-\infty}^\infty d\bar{\phi}_{2p} \delta\left(\epsilon - \frac{1}{2} \sum_{p=0}^{N-1} c_{2p+1} \phi_{2p+1}^2 - \frac{1}{2} \sum_{p=1}^N c_{2p} \bar{\phi}_{2p}^2\right) \delta\left(\sum_{p=0}^{N-1} c_{2p+1} \phi_{2p+1} - \sum_{p=1}^N c_{2p} \bar{\phi}_{2p}\right). \quad (43)$$

Rescaling the integration variables as $\phi_{2p+1} = \sqrt{\epsilon}x$ and $\bar{\phi}_{2p} = \sqrt{\epsilon}y$, we see that $f(\{c_n\})$ behaves as

$$f(\{c_n\}) \propto \epsilon^{N-\frac{3}{2}} = \left(\sum_{n=1}^{2N} c_n - c_{2N+1} \right)^{N-\frac{3}{2}}. \quad (44)$$

Note that a possible angular dependence of the scattering probability does not affect the threshold behavior in Eq. (44) because the scattering probability can be evaluated at $\phi_{2p+1} = 0$ and $\phi_{2p} = \pi$, which changes only the overall prefactor. For the case of two-particle scattering on a honeycomb lattice ($N = 2$, $c_{1\dots 4} = 1$, and $c_5 = c$) considered in Secs. III A and III B, we have $f(\{c_n\}) \propto \sqrt{\epsilon} = \sqrt{4-c}$. The inset in Fig. 4 shows that this is indeed the correct behavior near the threshold.

In the context of electron-electron scattering, $N \geq 2$. The $N = 1$ case corresponds to the situation when an electron scatters off some other object, e.g., a phonon. In this case, $f(\epsilon) \propto 1/\sqrt{\epsilon}$, i.e., the scattering rate diverges at the threshold.

E. Umklapp scattering on a 3D lattice

We now turn to N -particle scattering in 3D and show it provides a physical interpretation of the vanishing of the integral (1) with Bessel functions of *half-integer* orders, if Eq. (3) is satisfied but Eq. (2) is not. The Fermi surfaces will now be concentric spheres. Similar to the integral over circular Fermi surfaces found in (37), the scattering rate will now be proportional to the following integral over spherical Fermi surfaces (for $W_{\mathbf{k}_1, \mathbf{k}_2; \mathbf{k}'_1, \mathbf{k}'_2} = \text{const}$):

$$\begin{aligned} f(\{c_n\}) = \frac{1}{(4\pi)^{2N+1}} \prod_{n=1}^{2N} \int_0^\pi d\theta_n \sin\theta_n \int_0^{2\pi} d\phi_n \delta \left(\sum_{n=1}^{2N} (-1)^{n-1} c_n \sin\theta_n \cos\phi_n - c_{2N+1} \sin\theta_{2N+1} \cos\phi_{2N+1} \right) \\ \times \delta \left(\sum_{n=1}^{2N} (-1)^{n-1} c_n \sin\theta_n \sin\phi_n - c_{2N+1} \sin\theta_{2N+1} \sin\phi_{2N+1} \right) \\ \times \delta \left(\sum_{n=1}^{2N} (-1)^{n-1} c_n \cos\theta_n - c_{2N+1} \cos\theta_{2N+1} \right), \end{aligned} \quad (45)$$

where θ_n and ϕ_n are the polar and azimuthal angles of vector \mathbf{k}_n with magnitude $k_{F,n}$. Upon converting the δ functions to integrals over complex exponentials and swapping the order of integration, the integral becomes

$$\begin{aligned} f(\{c_n\}) = \frac{1}{(4\pi)^{2N+1}} \int_{-\infty}^{\infty} dx \int_{-\infty}^{\infty} dy \int_{-\infty}^{\infty} dz \prod_{n=1}^{2N} \int_0^\pi d\theta_n \sin\theta_n \int_0^{2\pi} d\phi_n e^{ix(\sum_{n=1}^{2N} (-1)^{n-1} c_n \sin\theta_n \cos\phi_n - c_{2N+1} \sin\theta_{2N+1} \cos\phi_{2N+1})} \\ \times e^{iy(\sum_{n=1}^{2N} (-1)^{n-1} c_n \sin\theta_n \sin\phi_n - c_{2N+1} \sin\theta_{2N+1} \sin\phi_{2N+1})} \\ \times e^{iz(\sum_{n=1}^{2N} (-1)^{n-1} c_n \cos\theta_n - c_{2N+1} \cos\theta_{2N+1})}. \end{aligned} \quad (46)$$

Exponentials with like arguments may once again be combined and subsequently integrated over, where now integrals over both azimuthal and polar angles are present. By converting the Cartesian coordinates to spherical coordinates $x = r \sin\vartheta \cos\varphi$, $y = r \sin\vartheta \sin\varphi$, and $z = r \cos\vartheta$, each of these $2N$ integrals may be written as

$$\begin{aligned} I_n &= \frac{1}{4\pi} \int_0^\pi d\theta_n \sin\theta_n \int_0^{2\pi} d\phi_n e^{\pm i c_n (x \sin\theta_n \cos\phi_n + y \sin\theta_n \sin\phi_n + z \cos\theta_n)} \\ &= \frac{1}{4\pi} \int_0^\pi d\theta_n \sin\theta_n \int_0^{2\pi} d\phi_n e^{\pm i c_n r (\sin\vartheta \sin\theta_n \cos(\phi_n - \varphi) + \cos\vartheta \cos\theta_n)}. \end{aligned} \quad (47)$$

The exponential terms may be separated and, due to 2π periodicity of the integrand in Eq. (47), the integral is reduced to

$$I_n = \frac{1}{2} \int_0^\pi d\theta_n \sin\theta_n e^{\pm i c_n r \cos\vartheta \cos\theta_n} J_0(c_n r \sin\vartheta \sin\theta_n). \quad (48)$$

Recalling the relation between the regular and spherical Bessel functions⁸,

$$j_\nu(z) = \frac{1}{2 \sin^\nu \vartheta} \int_0^\pi d\theta \sin^{\nu+1} \theta e^{iz \cos\vartheta \cos\theta} J_\nu(z \sin\vartheta \sin\theta), \quad (49)$$

we see that $I_n = j_0(c_n r)$, which leads us to the penultimate form

$$f(\{c_n\}) = \int_0^\infty dr r^2 \prod_{n=1}^{2N} j_0(c_n r) \frac{1}{2} \int_0^\pi d\vartheta \sin \vartheta e^{-ic_{2N+1} r \cos \vartheta \cos \theta_{2N+1}} \frac{1}{2\pi} \int_0^{2\pi} d\varphi e^{-ic_{2N+1} r \sin \vartheta \sin \theta_{2N+1} \cos \varphi}. \quad (50)$$

Applying Eq. (49) again, we arrive at the final form

$$f(\{c_n\}) = \int_0^\infty dr r^2 \prod_{n=1}^{2N+1} j_0(c_n r). \quad (51)$$

Recalling the additional definition relating spherical Bessel functions of order ν with regular Bessel functions of order $\nu + 1/2$

$$j_\nu(z) = \sqrt{\frac{\pi}{2z}} J_{\nu+1/2}(z), \quad (52)$$

it is clear that (51) can be rewritten in the same form as (1) with $\alpha = 3 - (2N + 1)/2$. If the polygonal constraint is not satisfied, the integral (45) vanishes independently from the values of θ_{2N+1} and ϕ_{2N+1} so that they may be set to $\pi/2$ and zero respectively. It is then clear that the same polygonal constraint is given by the inequality $c_{2N+1} \leq \sum_{n=1}^{2N} c_n$, which is the same as for the 2D case. This explains why the integral in Eq. (51) vanishes identically when the polygonal constraint is not satisfied. As in the 2D case, spherical Bessel functions of non-zero order occur due to the angular dependence of the scattering probability; however, we will not dwell on this issue here.

IV. HIGHER DIMENSIONALITIES

In the previous sections, we considered a special case of the integral (1) for $\alpha = 2$ which, in a physical interpretation, corresponds to the 2D case. In this section, we show that the same analysis can be extended for any even, integer dimensionality, i.e., for $\alpha = 2p$, $p = 1, 2, \dots$

Consider the following integral

$$f(\{c_n\}) = \int_0^\infty d\rho \rho^{2p-1} \prod_{n=1}^{M>1} J_0(c_n \rho). \quad (53)$$

Applying the same transformations as before, we obtain

$$\begin{aligned} f(\{c_n\}) &= \frac{1}{(2\pi)^M} \prod_{n=1}^{M-1} \int_0^{2\pi} d\phi_n \int_{-\infty}^\infty dx \int_{-\infty}^\infty dy (x^2 + y^2)^{p-1} e^{ix(\sum_{n=1}^{M-1} c_n \cos \phi_n - c_M \cos \phi_M)} e^{iy(\sum_{n=1}^{M-1} c_n \sin \phi_n - c_M \sin \phi_M)} \\ &= \frac{1}{(2\pi)^M} \prod_{n=1}^{M-1} \int_0^{2\pi} d\phi_n \int_{-\infty}^\infty dx \int_{-\infty}^\infty dy \sum_{l=0}^{p-1} C_{p-1}^l x^{2l} y^{2(p-1-l)} e^{ix(\sum_{n=1}^{M-1} c_n \cos \phi_n - c_M \cos \phi_M)} \\ &\quad \times e^{iy(\sum_{n=1}^{M-1} c_n \sin \phi_n - c_M \sin \phi_M)}, \end{aligned} \quad (54)$$

where we used the binomial expansion at the last step with $C_n^m = n!/m!(n-m)!$ being the binomial coefficient. Relabeling $x_M = c_M \cos \phi_M$ and $y_M = c_M \sin \phi_M$, we rewrite x^{2l} as the $(2l)$ th derivative of the first exponential factor $x^{2l} \dots = (-)^l \partial_{x_M}^{2l} \dots$, and similarly for $y^{2(p-1-l)}$. Integrating over x and y , we obtain

$$f(\{c_n\}) = \frac{1}{(2\pi)^M} \prod_{n=1}^{M-1} \int_0^{2\pi} d\phi_n \sum_{l=0}^{p-1} C_{p-1}^l (-)^{p-1} \partial_{x_M}^{2l} \partial_{y_M}^{2(p-1-l)} \delta\left(\sum_{n=1}^{M-1} c_n \cos \phi_n - x_M\right) \delta\left(\sum_{n=1}^{M-1} c_n \sin \phi_n - y_M\right). \quad (55)$$

If the polygonal constraint is not satisfied, each of the δ -functions in the equation above vanishes identically along with all its derivatives.

As an example, consider the integral (53) with $p = 2$ and $M = 7$ (the smallest M for which the integral with $\alpha = 4$ is convergent)

$$f(c) = \int_0^\infty d\rho \rho^3 J_0^6(\rho) J_0(c\rho). \quad (56)$$

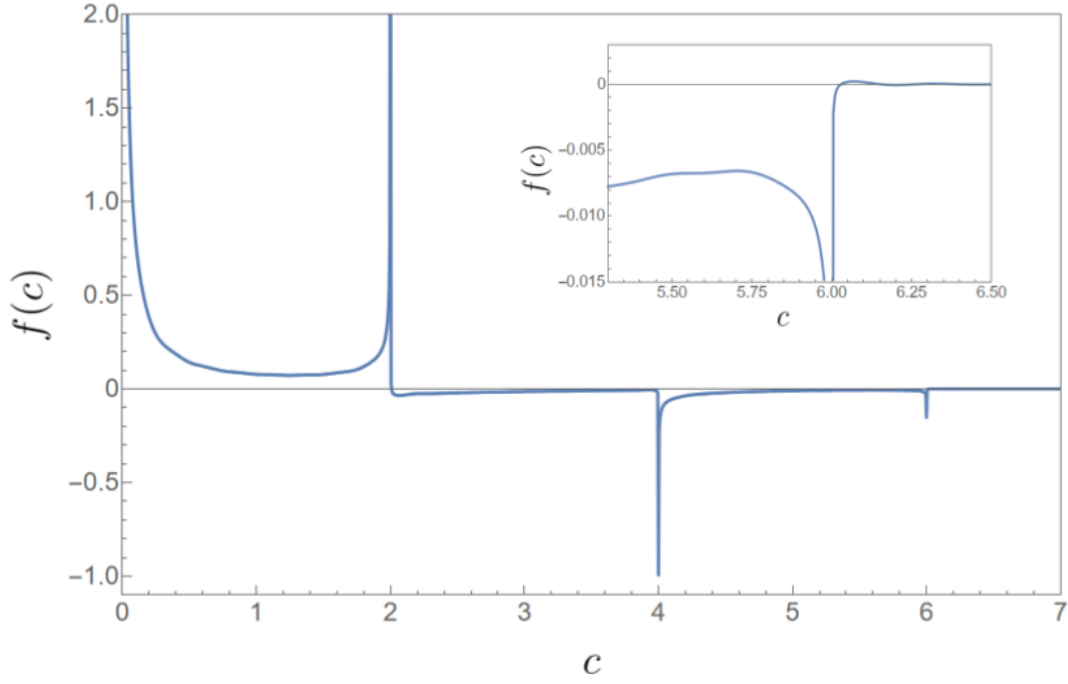


Figure 6: Numerical result for the integral (56).

With all $\nu_n = 0$ and $\alpha = 4$, the charge neutrality condition (3) is satisfied with $m = 2$, and thus the integral vanishes when the polygonal constraint (2) is not satisfied, namely for $c > 6$. The numerical result for Eq. (56) is shown in Fig. 6, where it is seen $f(c)$ is indeed nonzero only when $c < 6$, within a reasonable numerical accuracy.

The analysis above can be generalized for Bessel functions of arbitrary integer orders, in which case

$$f(\{c_n\}) = \int_0^\infty d\rho \rho^{2p-1} \prod_{n=1}^{M-1} \int_0^{2\pi} \frac{d\phi_n}{2\pi i^{\nu_n}} e^{i \sum_{n=1}^{M-1} (c_n \rho \cos \phi_n + \nu_n \phi_n)} \frac{(-1)^{\nu_M}}{2\pi i^{\nu_M}} \int_0^{2\pi} d\varphi e^{i(-c_M \rho \cos \varphi + \nu_M \varphi)}. \quad (57)$$

Upon transforming to Cartesian coordinates and shifting the variables as $\varphi \rightarrow \varphi - \phi_M$ and $\phi_n \rightarrow \phi_n - \varphi$, the integral is reduced to

$$f(\{c_n\}) = e^{-i\nu_M \phi_M} \frac{(-1)^{\nu_M}}{2\pi i^{\nu_M}} \prod_{n=1}^{M-1} \int_0^{2\pi} \frac{d\phi_n}{2\pi i^{\nu_n}} e^{i \sum_{n=1}^{M-1} \nu_n \phi_n} \times \int_{-\infty}^\infty dx \int_{-\infty}^\infty dy (x^2 + y^2)^{p-1} e^{ix(\sum_{n=1}^{M-1} c_n \cos \phi_n - c_M \cos \phi_M)} e^{iy(\sum_{n=1}^{M-1} c_n \sin \phi_n - c_M \sin \phi_M)} e^{i(\nu_M - \sum_{n=1}^{M-1} \nu_n) \varphi}, \quad (58)$$

If the charge neutrality condition (3) is satisfied with $\alpha = 2p = 2m$ and $m = 1, 2, 3, \dots$, the last phase factor is reduced to unity, and the ensuing δ -functions (and/or their derivatives) enforce the polygonal constraint (2).

We need to stress that α being even is a sufficient but not necessary condition for the integral to vanish, if the polygonal constraint is not satisfied. It is just that for α even, the δ -functions appear explicitly. However, the charge neutrality condition (3) may be satisfied even for irrational and complex ν_n and α , when the integral cannot be expressed in terms of δ -functions. Recall from Eq. (4) that when the charge neutrality condition (3) is satisfied while the polygonal constraint (2) is not, the integral vanishes due to zeros in the following function

$$\frac{1}{\Gamma(\nu_M - \mu/2 + 1)} = \frac{1}{\Gamma(-m + 1)}; \quad m = 1, 2, 3, \dots \quad (59)$$

V. CONCLUSIONS

Integrals of products of Bessel functions have been studied for well over 150 years, and yet their properties and emergence in a variety of seemingly unrelated physical problems do not cease to amaze. Of particular interest is how the vanishing of such

integrals are linked to two constraints, the polygonal constraint relating the argument coefficients to sides of a polygon, Eq. (2), and what we have dubbed as the charge neutrality condition, Eq. (3). Given that the integral is convergent, if Eq. (3) is satisfied while Eq. (2) is not, the integral is identically equal to zero.

Examples of such integrals appear in a context of great interest in condensed matter physics, namely the density of states and mutual scattering rate of electrons moving on a 2D or 3D lattice. The integrals that appear in this context involve Bessel functions of integer orders, and δ -functions may be employed to show intuitively why the integrals vanish when satisfying the constraints. For the model discussed, the absence of an umklapp scattering channel on a Fermi surface smaller than a critical value corresponds to the breaking of the polygonal constraint. The integral that gives the corresponding scattering rate goes from zero to a finite value, with a concomitant discontinuity in the derivative. We also showed that the approach based on δ -functions allows one to prove the vanishing of integrals of products of Bessel functions of arbitrary integer orders and in even dimensionalities α , as defined in Eq. (1). We expect these types of integrals to continue to appear in new and interesting settings, and as they emerge, further insights are likely to emerge alongside.

VI. SUPPLEMENTARY MATERIAL

In the Supplementary Material, we present a detailed derivation of the umklapp scattering rate on a 2D honeycomb lattice. We begin in Sec. I with a brief review of single-electron dynamics on a 2D honeycomb lattice in the nearest-neighbor-hopping approximation. We proceed in Sec. IIA to define the on-site Hubbard Hamiltonian for electron-electron interactions in terms of the low energy electron operators presented in Sec. I. Via the Boltzmann formalism and Fermi's Golden Rule, we derive the umklapp scattering rate in Sec. IIB. In Sec. III we show how additional discontinuities in the derivative of $f(c)$ appear for a specific example.

ACKNOWLEDGMENTS

We thank A. Chubukov, I. Gaiur, T. Kiliptari, S. Majumdar, V. Roubtsov, and V. Schechtman for stimulating discussions. This work was initiated at the Aspen Center for Physics, which is supported by National Science Foundation grant PHY-2210452, and supported by National Science Foundation via grant DMR-2224000. D. L. M. also acknowledges the hospitality of the Kavli Institute for Theoretical Physics, Santa Barbara, supported by the NSF grants PHY-1748958 and PHY-2309135.

REFERENCES

- ¹G. Watson, *A Treatise on the Theory of Bessel Functions*, 2nd ed. (Cambridge University Press, Cambridge, England, 1944).
- ²A. D. Jackson and L. C. Maximon, "Integrals of Products of Bessel Functions," *SIAM Journal on Mathematical Analysis* **3**, 446–460 (1972).
- ³R. Mehrem, J. T. Londergan, and M. H. Macfarlane, "Analytic expressions for integrals of products of spherical Bessel functions," *Journal of Physics A: Mathematical and General* **24**, 1435–1453 (1991).
- ⁴R. Mehrem and A. Hohenegger, "A generalization for the infinite integral over three spherical Bessel functions," *Journal of Physics A: Mathematical and Theoretical* **43**, 455204 (2010).
- ⁵R. Mehrem, "Analytical evaluation of an infinite integral over four spherical Bessel functions," *Applied Mathematics and Computation* **219**, 10506–10509 (2013).
- ⁶S. N. Majumdar and E. Trizac, "When Random Walkers Help Solving Intriguing Integrals," *Physical Review Letters* **123**, 020201 (2019).
- ⁷A. P. Prudnikov, Y. A. Brychkov, and O. I. Marichev, *Integrals and Series: Special functions* (CRC Press).
- ⁸N. Sonine, "Recherches sur les fonctions cylindriques et le développement des fonctions continues en séries," *Mathematische Annalen* **16**, 1–80 (1880).
- ⁹J. Nicholson, "Generalisation of a theorem due to Sonine," *The Quarterly Journal of Pure and Applied Mathematics* **48**, 321–329 (1920).
- ¹⁰N. W. Ashcroft and N. D. Mermin, *Solid State Physics* (Holt, Rinehart and Winston, New York, NY, 1976).
- ¹¹L. Mihály and M. Martin, *Solid State Physics: Problems and Solutions* (WILEY-VCH Verlag, 2009).
- ¹²E. M. Lifshitz and L. P. Pitaevskii, *Physical Kinetics, Course of Theoretical Physics*, v. X (Butterworth-Heinemann, Burlington, 1981).
- ¹³A. H. Castro Neto, F. Guinea, N. M. R. Peres, K. S. Novoselov, and A. K. Geim, "The electronic properties of graphene," *Reviews of Modern Physics* **81**, 109–162 (2009).